Journal of Sound and Vibration (2002) **255**(4), 793–803
doi:10.1006/jsvi.2001.4170, available online at http://www.idealibrary.com on IDEAL®

FREE VIBRATION OF CONTINUOUS SLAB-BEAM SKEWED BRIDGES

S. MALEKI

Department of Civil Engineering and Construction, Bradley University, Peoria, IL 61625, *U.S.A.*

(*Received* 2 *April* 2001, *and in final form* 31 *October* 2001)

1. INTRODUCTION

Slab-beam steel bridges consist of a concrete deck spanning over steel stringers which can have composite action with the deck concrete. An economical range of span for this type of bridge can extend up to 15 m with rolled steel sections. Higher spans can be covered by continuous construction. A typical plan view of a continuous skewed bridge is shown in Figure 1. The cross-sectional view showing end cross-frames are shown in Figure 2. Figure 3 shows a typical elastomeric bearing detail. Details shown in Figures 2 and 3 are standard in the state of Illinois [1].

The period of vibration and inertial forces induced in a bridge structure depend on the stiffness of supporting members, such as end-diaphragms and elastomeric bearings, in two non-orthogonal directions. Inertial forces resulting from an earthquake are transferred from the deck to cross-frames at the end of the span and then to the bearings. The cross-frames affect the lateral stiffness of the bridge in the direction of skew, and elastomeric bearings affect the stiffness of the bridge in the longitudinal direction.

In this paper, based on stiffness of elastomeric bearings and cross-frames, the dynamic behavior of symmetrical continuous skewed bridges will be studied. Equations for the determination of the translational periods of free vibration will be derived. In addition, correlation factors relating the periods of a straight bridge to those of a skewed bridge with the same properties are derived.

It is assumed that the concrete deck is rigid in its own plane. Turkington *et al.* [2] claim that this assumption is valid for decks with length-to-width (aspect) ratios of less than 8. This is because the in-plane deck stiffness is very high in comparison with cross-frame and elastomeric bearing stiffnesses. Although the overall span of continuous bridges can be very long, only the aspect ratio of each individual span will be the determining factor for deck stiffness. For slab-girder bridges, each span is limited by the economical range, and usually, does not exceed 20 m.

Zahrai *et al.* [3] indicate that end-diaphragms, in the form of a single channel section connecting the girders, perform poorly in earthquakes. This is due to their flexibility and lack of connection to the lower part of the girder. Hence, the use of end cross-frames, as shown in Figure 2, is recommended for bridges in seismic zones. In addition, they prove that intermediate diaphragms do not affect the seismic behavior. In this paper, only the effect of end-diaphragms in the form of cross-frames is considered.

Skewed bridges have vibrational modes that do not uncouple in orthogonal directions. This means that, for a typical elastically supported skewed bridge as shown in Figure 1, the translational modes of free vibration are not in the X or Y directions. In fact, they are closer

0022-460X/02/$35.00

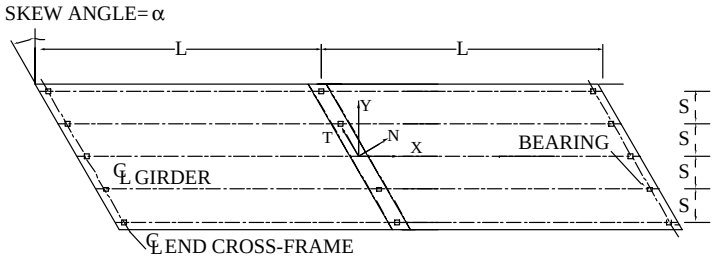

Figure 1. Bridge plan view.

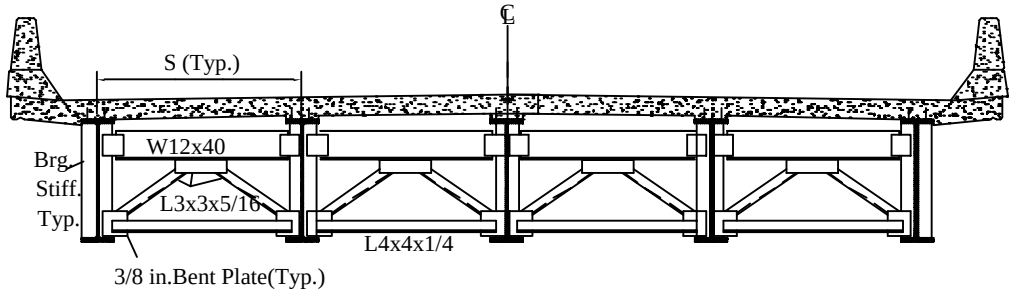

Figure 2. End-diaphragm detail.

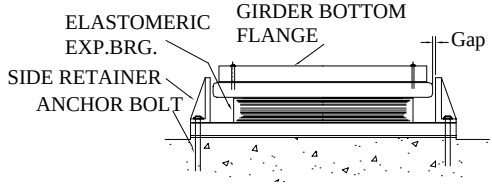

Figure 3. Elastomeric bearing detail.

to the *N* and *T* directions, i.e., normal and tangent to the abutments. Currently, AASHTO [4] proposes the use of the multimode spectral analysis method for bridges in which coupling occurs in more than one of the three coordinate directions within each mode of vibration. Linear dynamic analysis is also the minimum requirement for skewed bridges according to ATC-32, section C3.21.4 [5]. In this paper, a simple method for obtaining the translational periods of free vibration is given without resorting to complicated analysis. The results are verified using the SAP2000 [6] program and a three-dimensional finite element model. The behavior of single-span skewed bridges, supported elastically, has been studied by Maleki [7, 8]. This is an extension of the work to cover continuous bridges.

2. FREE VIBRATION ANALYSIS

A typical symmetric continuous skewed slab-girder bridge, as shown in Figure 1, is considered for analysis. The bulk of the mass in a slab-girder bridge is at the deck level. In the event of an earthquake, the inertial loads will be generated at the deck. These forces have

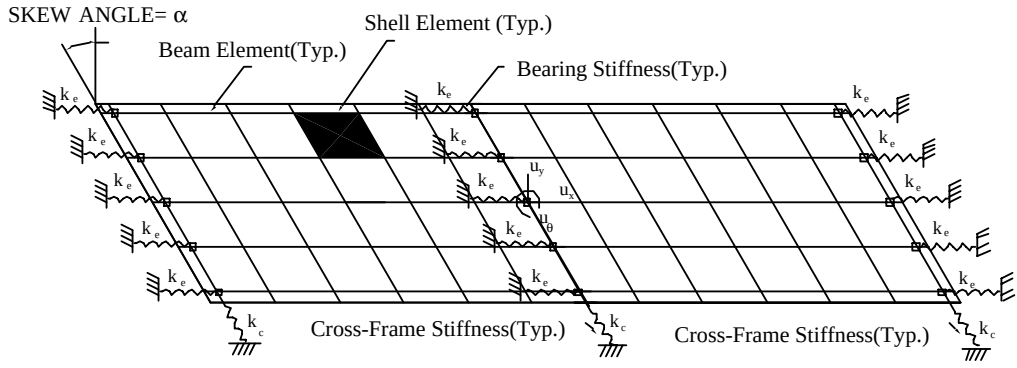

Figure 4. Bridge finite element model.

to pass through the end-diaphragms and bearings to reach the substructure and finally the ground. As a result, the stiffness of all these components will affect the dynamic behavior of the bridge. The in-plane stiffness of the deck is very high in comparison with the end-diaphragms and it is assumed to be rigid. This means that all points on the deck will displace equally.

A skewed bridge is a parallelogram in plan. The center of mass is chosen as the origin and two sets of axes are defined at this point. The X–Y axes are in the longitudinal and transverse directions, and N–T axes are normal and parallel to the supports. Note that, due to symmetry, the center of mass and stiffness coincide, and hence, translational loads at the center of mass do not cause any torsional loading. This is true regardless of number of spans, as long as, symmetry in geometry and support stiffness is preserved.

A three-dimensional finite element model of the bridge and the three degrees of freedom (d.o.f.) at the center of mass are shown in Figure 4. The springs k_e represent the stiffness of elastomeric bearing in the X direction, and springs k_c represent the total lateral stiffness of the cross-frames in the T direction. Let M and I_o represent the total mass and the mass moment of inertia of the bridge superstructure. These are assumed to be concentrated at the center of mass. Assuming zero damping, the equation of motion for free vibration of the model bridge in Figure 4 can be written as follows:

$$\begin{bmatrix} M & 0 & 0 \\ 0 & M & 0 \\ 0 & 0 & I_0 \end{bmatrix} \begin{Bmatrix} \ddot{u}_x \\ \ddot{u}_y \\ \ddot{u}_\theta \end{Bmatrix} + \begin{bmatrix} K_{xx} & K_{xy} & K_{x\theta} \\ K_{yx} & K_{yy} & K_{y\theta} \\ K_{\theta x} & K_{\theta y} & K_{\theta\theta} \end{bmatrix} \begin{Bmatrix} u_x \\ u_y \\ u_\theta \end{Bmatrix} = \begin{Bmatrix} 0 \\ 0 \\ 0 \end{Bmatrix}, \tag{1}$$

where K_{xx} and K_{yy} are the summation of all transformed stiffness in the X and Y direction respectively; $K_{\theta\theta}$ is derived from rotational equilibrium and it is equal to

$$K_{\theta\theta} = \Sigma(k_c e_x^2 + k_e e_y^2), \tag{2}$$

where "e" denotes the eccentricity of springs with respect to center of mass in a direction perpendicular to the line of action of each spring. Other stiffness terms are coupled terms.

The stiffness matrix in equation (1) above is diagonal for a straight bridge and all the non-diagonal terms are equal to zero. As a result, a non-skewed bridge will have its fundamental mode of vibration in the X (or Y) direction only. Ground motion in the X (or Y) direction would cause only lateral displacement in the X (or Y) direction. The bridge

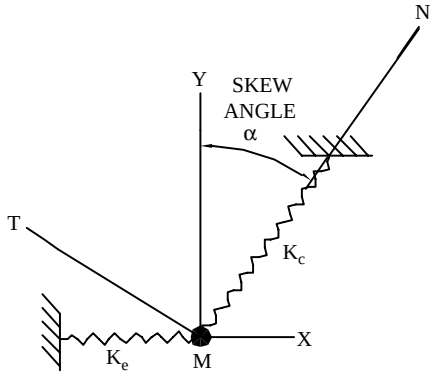

Figure 5. Lumped mass analysis model.

would experience no torsional motion unless the base motion includes rotation about a vertical axis.

For a skewed bridge with center of mass and stiffness coinciding, the torsional mode uncouples, but the translational modes are coupled. Therefore,

$$K_{\theta x} = K_{x\theta} = K_{\theta y} = K_{y\theta} = 0. \tag{3}$$

The period of vibration for the uncoupled torsional mode is

$$T = 2\pi \sqrt{\frac{I_0}{K_{\theta\theta}}}. \tag{4}$$

This paper is mainly concerned with translational modes of vibration. To illustrate the nature of the coupled translational modes of vibration, a simplified model of the bridge can be made with only two springs, K_e and K_c, and a mass, M, as shown in Figure 5. Spring K_e represents elastomer's total shear stiffness in the X direction, and spring K_c represents cross-frame's total stiffness in the T direction. Transforming the local co-ordinates along N- and T-axis of the K_c spring to the global X and Y co-ordinates the stiffness terms in equation (1) are

$$K_{xx} = K_e + K_c \sin^2 \alpha, \quad K_{xy} = K_c \sin \alpha \cos\ \alpha = K_{yx}, \quad K_{yy} = K_c \cos^2 \alpha. \tag{5–7}$$

Solving the eigenvalue problem leads to periods of free vibration of the system:

$$T = \sqrt{8\pi^2 M / [(K_e + K_c) \pm \sqrt{(K_e + K_c)^2 - 4K_e K_c \cos^2 \alpha}]}. \tag{8}$$

It is obvious that the periods of vibration are coupled and depend on both spring stiffness, K_e and K_c. For the case of a straight bridge α–is equal to zero and (8) reduces to

$$T_0 = \sqrt{\frac{8\pi^2 M}{[(K_e + K_c) \pm (K_e - K_c)]}} = 2\pi \sqrt{\frac{M}{K_e}} \quad \text{and} \quad 2\pi \sqrt{\frac{M}{K_c}}, \tag{9}$$

which are familiar uncoupled results as expected. Introducing a non-dimensional parameter as $\beta = K_e/K_c$, equation (8) can be rewritten as

$$T = \sqrt{8\pi^2 M / K_c [(1 + \beta) \pm \sqrt{(1 + \beta)^2 - 4\beta \cos^2 \alpha}]}. \tag{10}$$

This is the exact equation for the period of vibration of a skewed bridge. Substituting zero for parameter α, the period for a straight bridge is derived as

$$T_0 = \sqrt{8\pi^2 M / K_c[(1+\beta) \pm (1-\beta)]}. \tag{11}$$

Note that the elastomer's stiffness is omni-directional. However, as the detail in Figure 3 shows, the retainer plate prevents the displacement of the elastomer in any other direction except the longitudinal direction. The retainer's stiffness and elastomer's stiffness are like springs attached in parallel. The equivalent stiffness is the sum of the two, and the retainer being much stiffer actually dominates. Moreover, this combined stiffness is in series with abutment or pier stiffness.

In the analytical models, all these springs were replaced with one spring (i.e., K_c). This shows the effect of the cross-frame, which is the dominant part for most bridges. However, if one desires more accuracy, the stiffness of substructure and retainer and all of the above can be added to give an equivalent K_c. In that case, the derived formulas are still valid.

Moreover, the inclusion of K_e in the development of formulas is purely mathematical. For continuous bridges, at least one end of the girder is pin supported. This will cause the total stiffness in the longitudinal direction to approach infinity. Hence, the results for the case of $\beta = \infty$ should be used.

It should be noted that varying the geometry (span or width) of the bridge only changes the mass, M, in the numerator of the above equations. The relationship between mass and period is well known, and is not considered as a parameter in this study. The effects of other parameters are explored in the next section.

3. CORRELATION BETWEEN SKEWED AND STRAIGHT BRIDGE PERIODS

To arrive at a correlation factor between the periods of a skewed bridge and a straight bridge with similar properties, one can divide equation (10) by equation (11). Considering the $\pm$ sign in the denominators, four factors are obtained as follows:

$$R_1 = \frac{T}{T_0} = \sqrt{[(1+\beta) + \sqrt{(1-\beta)^2}]/[(1+\beta) - \sqrt{(1+\beta)^2 - 4\beta\cos^2\alpha}]}, \tag{12}$$

$$R_2 = \frac{T}{T_0} = \sqrt{[(1+\beta) - \sqrt{(1-\beta)^2}]/[(1+\beta) - \sqrt{(1+\beta)^2 - 4\beta\cos^2\alpha}]}, \tag{13}$$

$$R_3 = \frac{T}{T_0} = \sqrt{[(1+\beta) + \sqrt{(1-\beta)^2}]/[(1+\beta) + \sqrt{(1+\beta)^2 - 4\beta\cos^2\alpha}]}, \tag{14}$$

$$R_4 = \frac{T}{T_0} = \sqrt{[(1+\beta) - \sqrt{(1-\beta)^2}]/[(1+\beta) + \sqrt{(1+\beta)^2 - 4\beta\cos^2\alpha}]}. \tag{15}$$

The function R_1 can be described as the ratio of the first period of a skewed bridge to the second period of a straight bridge. Likewise, R_2 is the ratio of the first period of a skewed bridge to the first period of a straight bridge, R_3 is the ratio of second periods, and R_4 is the ratio of second period to first period.

Figures 6–9 are the plots of the above four correlation factors versus β respectively. In addition, each graph shows the variation of skew angle from 0 to 60°.

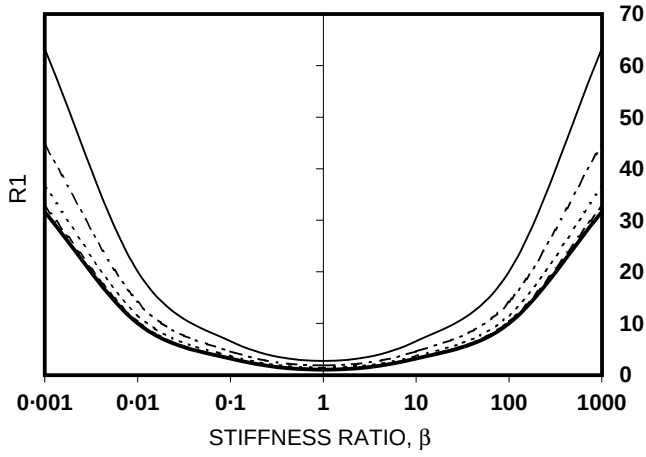

Figure 6. Correlation factor R_1 versus stiffness ratio β: ——, $\alpha = 0$; – – – – –, $\alpha = 15$; ·····, $\alpha = 30$; –·–·–·– $\alpha = 45$; ——, $\alpha = 60$.

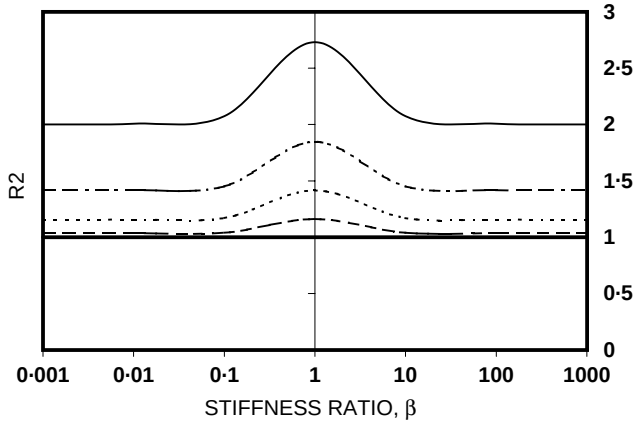

Figure 7. Correlation factor R_2 versus stiffness ratio β: ——, $\alpha = 0$; – – – – –, $\alpha = 15$; ·····, $\alpha = 30$; –·–·–·– $\alpha = 45$; ——, $\alpha = 60$.

Referring to Figure 6, the author has found that R_1 can be approximated with a good accuracy with the functions

$$R_1 \approx \sqrt{\beta}/\cos\alpha \quad \text{for } \beta \geqslant 10 \quad \text{and} \quad R_1 \approx 1/\sqrt{\beta}\cos\alpha \quad \text{for } \beta \leqslant 0{\cdot}10. \qquad (16, 17)$$

Compared to equation (12), the maximum error of these functions occur at $\beta = 0{\cdot}1$ or 10. The maximum percentage of error ranges from 0·4%, for $\alpha = 15$, to 3·6% for $\alpha = 60$ at these points. These errors reduce to zero when β approaches 1000 or 0·001. Hence, it is concluded that equations (16) and (17) are in excellent agreement with the exact values in the specified β range. The range in equation (16) is the practical range of β for pinned bearings in the longitudinal direction, and the range in equation (17) is applicable to elastomeric bearing supports.

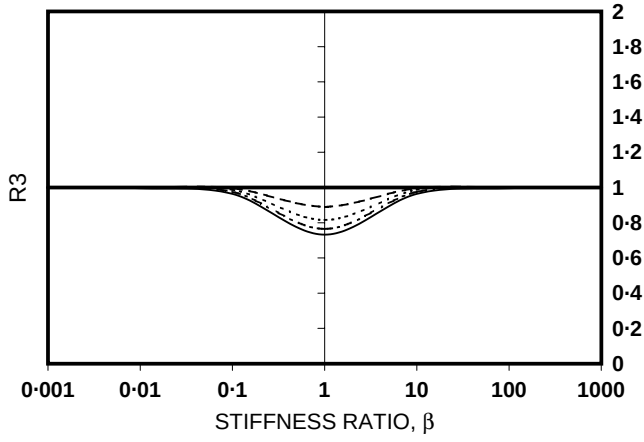

Figure 8. Correlation factor R_3 versus stiffness ratio β: ——, $\alpha = 0$; – – – – –, $\alpha = 15$; ·····, $\alpha = 30$; –·–·–·–·, $\alpha = 45$; ——, $\alpha = 60$.

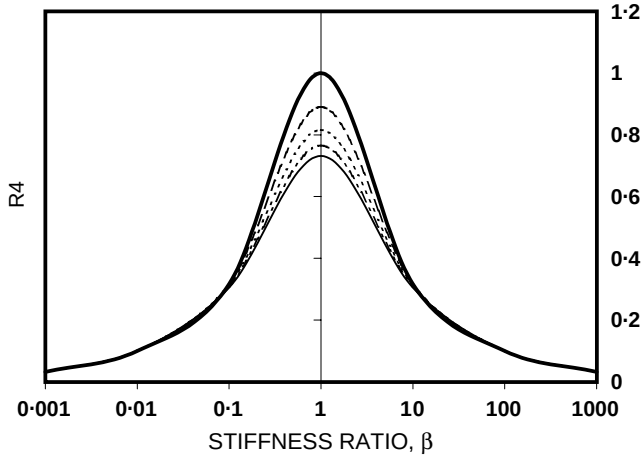

Figure 9. Correlation factor R_4 versus stiffness ratio β: ——, $\alpha = 0$; – – – – –, $\alpha = 15$; ·····, $\alpha = 30$; –·–·–·–·, $\alpha = 45$; ——, $\alpha = 60$.

Likewise, Figure 7 shows the relationship between the first periods. For practical ranges of β, the function R_2 can be approximated with

$$R_2 \approx 1/\cos\alpha \quad \text{for} \quad \beta \leqslant 0{\cdot}1, \quad \beta \geqslant 10; \tag{18}$$

the maximum error for this approximation is 3·6%.

Refering to Figure 8, the function R_3 can be approximated with 3·6% maximum error as

$$R_3 \approx 1 \quad \text{for } \beta \leqslant 0{\cdot}1, \ \beta \geqslant 10 \tag{19}$$

and the function R_4, in Figure 9, can be approximated, with 3·6% maximum error, as

$$R_4 \approx \sqrt{1/\beta} \quad \text{for } \beta \geqslant 10 \quad \text{and} \quad R_4 \approx \sqrt{\beta} \quad \text{for } \beta \leqslant 0{\cdot}1 \tag{20, 21}$$

which are actually the values of function R_4 when $\alpha = 0$, i.e., a straight bridge.

For practical applications, the correlation factors R_2 and R_3 are simpler to use than R_1 and R_4, and cover all practical ranges of β. Having the first and second periods of a straight bridge, one can arrive at the periods of a skewed bridge by multiplying them by the corresponding factor. In the next section, these properties are examined further by solving a numerical example and comparing the results with finite element analysis.

4. NUMERICAL EXAMPLES

A two-span continuous skewed bridge as shown in Figure 1 is considered for analysis. The periods of vibration based on the theoretical development in the previous sections and estimates based on the correlation factors are calculated and compared here.

The mass of the bridge is estimated to be 130 000 kg. The lateral stiffness of each cross-frame, with detail as depicted in Figure 3, is found to be equal to 500 kN/mm. For a two-span continuous bridge the sum of three cross-frame stiffness is equal to $K_c = 1500$ kN/mm. A typical shear stiffness for an ordinary elastomeric bearing for this bridge is 1·0 kN/mm. Hence, for 15 bearings a total stiffness of $K_e = 15$ kN/mm is assumed. Note that this is only an assumption. In actual practice at least one set of bearings are pinned; which increases the stiffness to infinity in the longitudinal direction. Using these values, for a skew angle of $\alpha = 60$, the exact translational periods of vibration can be obtained as

$$\beta = \frac{K_e}{K_c} = \frac{15}{1500} = 0{\cdot}01. \tag{22}$$

Substituting this in equation (10) gives

$$T = \sqrt{\frac{8\pi^2 M}{K_c[(1+\beta) \pm \sqrt{(1+\beta)^2 - 4\beta\cos^2\alpha}]}} = \sqrt{\frac{10{\cdot}26 \times 10^6}{1{\cdot}5 \times 10^9[1{\cdot}01 \pm (1{\cdot}005)]}} \tag{23}$$

and upon simplification,

$$T_1 = 1{\cdot}174 \quad \text{and} \quad T_2 = 0{\cdot}0583 \text{ s}, \tag{24}$$

which are the two translational periods of vibration.

These same periods could have been estimated by using the correlation factors R_2 and R_3 as given by equations (18) and (19). First, we calculate the uncoupled periods of a straight bridge with the same properties from equation (9):

$$T_{01} = 2\pi\sqrt{\frac{M}{K_e}} = 2\pi\sqrt{\frac{130\,000}{15 \times 10^6}} = 0{\cdot}585 \text{ s}, \quad T_{02} = 2\pi\sqrt{\frac{M}{K_c}} = 2\pi\sqrt{\frac{130\,000}{1{\cdot}5 \times 10^9}} = 0{\cdot}0585 \text{ s}. \tag{25, 26}$$

Then we apply the correlation factors to obtain the periods of skewed bridge as:

$$T_1 = R_2 \times T_{01} = \left(\frac{1}{\cos\alpha}\right)(0{\cdot}585) = 1{\cdot}170 \text{ s}, \qquad T_2 = R_3 \times T_{02} = (1)\left(0{\cdot}0585\right) = 0{\cdot}0585 \text{ s}. \tag{27, 28}$$

These are in good agreement with the exact values of equation (24). The results for other skew angles are calculated and shown in Table 1.

To compare the estimated values derived above, with an actual finite element model, a three-dimensional model of the bridge is made with program SAP2000 [5], as shown in

TABLE 1

Free vibration periods comparison, elastomeric bearings

Analysis method	Skew angle	Total K_e (kN/mm)	Total K_c (kN/mm)	$\beta = K_e/K_c$	Period T_1 (s)	Period T_2 (s)
SAP2000	0	15	1500	0·01	0·584	0·0584
Equation (10)					0·585	0·0585
R_2 and R_3 estimates					0·585	0·0585
SAP2000	15	15	1500	0·01	0·605	0·0584
Equation (10)					0·606	0·0585
R_2 and R_3 estimates					0·605	0·0585
SAP2000	30	15	1500	0·01	0·676	0·0584
Equation (10)					0·676	0·0584
R_2 and R_3 estimates					0·675	0·0585
SAP2000	45	15	1500	0·01	0·829	0·0583
Equation (10)					0·829	0·0583
R_2 and R_3 estimates					0·827	0·0585
SAP2000	60	15	1500	0·01	1·173	0·0582
Equation (10)					1·174	0·0583
R_2 and R_3 estimates					1·170	0·0585

TABLE 2

Free vibration periods comparison, pin supported condition

Analysis method	Skew angle	Total K_e (kN/mm)	Total K_c (kN/mm)	$\beta = K_e/K_c$	Period T_1 (s)	Period T_2 (s)
SAP2000	0	1·5E6	1500	1000	0·0584	0·0018
Equation (10)					0·0585	0·0018
R_2 and R_3 estimates					0·0585	0·0018
SAP2000	15	1·5E6	1500	1000	0·0605	0·0018
Equation (10)					0·0605	0·0018
R_2 and R_3 estimates					0·0605	0·0018
SAP2000	30	1·5E6	1500	1000	0·0675	0·0018
Equation (10)					0·0675	0·0018
R_2 and R_3 estimates					0·0675	0·0018
SAP2000	45	1·5E6	1500	1000	0·0827	0·0018
Equation (10)					0·0827	0·0018
R_2 and R_3 estimates					0·0827	0·0018
SAP2000	60	1·5E6	1500	1000	0·117	0·0018
Equation (10)					0·117	0·0018
R_2 and R_3 estimates					0·117	0·0018

Figure 4. The total mass of 130 000 kg is assumed to be distributed uniformly over the concrete deck. The deck is modelled with shell elements of 0·19 m thickness. The girders are W36 × 230 and are rigidly attached to the deck slab. All joints are constrained in the deck slab plane to perform as a rigid diaphragm. The end of the girders are attached to

longitudinal springs that represent the elastomeric bearing's shear stiffness. There are also springs in the transverse T direction that simulate the stiffness of the cross-frames. The latter is modelled using the non-linear link elements of SAP2000. This is the only way one can model skewed springs in the T direction with this program. However, the non-linear portion of the spring is not activated. Both of these springs are attached to the ground, i.e., the substructure is assumed to be rigid. Zero damping is assumed in the free vibration analysis. The analyses results are shown in Table 1 and compared to previous values. In addition, estimates of the translational periods using the R_2 and R_3 factors, described in the previous section, are also given. It is clear that the simplified model results are in excellent agreement with the SAP2000 results. Hence, the validity of the theoretical development for the periods of vibration is verified. The slight discrepancy in some cases is due to the finite element model and can be eliminated with a finer mesh.

As a second example, consider the free vibration analysis of a pin-supported skewed bridge. An analysis is made which assumes a β value of 1000. This is very close to a pin-supported condition for the bearing. For a pin-supported bridge, the K_e spring, in reality, represents the out-of-plane stiffness of the abutment; this is due to infinite stiffness of the hinged bearings.

The results are summarized in Table 2 and are in good agreement with theoretical models. Note that, due to high stiffness in the longitudinal direction, the second period is very small.

5. CONCLUSIONS

For a symmetric continuous skewed bridge, supported on elastomeric bearings, and having cross-frames at ends, this study concluded that the exact periods for translational modes of vibration can be calculated from equation (10). These periods depend on elastomer and cross-frame stiffness and skew angle. The span or width of the bridge affects the mass, and the square root of mass is proportional to period. Since the relationship is well known, mass or span length has not been considered as a parameter in this study.

With the aid of correlation factors derived in this study, estimates of the translational periods of a continuous skewed bridge can be obtained from the period of a straight bridge with the same characteristics. The first period of a skewed bridge is obtained by dividing the period of a straight bridge by the factor $\cos\alpha$ as given by equation (18). The second period of a skewed bridge is equal to that of a straight bridge as indicated by equation (19). It has been shown that the estimates are in excellent agreement with exact values for practical ranges of support stiffness. The findings are valid regardless of the number of spans. However, the limitation of symmetry in geometry and support stiffness has to be satisfied.

REFERENCES

1. Illinois Department of Transportation 1999 *Bridge Manual. Springfield, Illinois.*
2. A. J. Turkington, A. J. Carr, N. Cooke and P. J. Moss 1989 *American Society of Civil Engineers Journal of Structural Engineering* **115**, 3000–3016. Seismic design of bridges on lead–rubber bearings.
3. S. M. Zahrai and M. Bruneau 1998 *American Society of Civil Engineers Journal of Structural Engineering* **124**, 938–947. Impact of diaphragms on seismic response of straight slab-on-girder bridges.
4. American Association of State Highway and Transportation Officials 1998 *AASHTO-LRFD. Washington, DC*. Bridge design specification.
5. Applied Technology Council 1996 *ATC*-32 Redwood City, California. Improved seismic design criteria for California bridges: provisional recommendations.

6. COMPUTERS and STRUCTURES, Inc. 2000 *SAP*2000 *Version* 7.4. *Berkeley*, *CA*, *USA*. Integrated structural analysis and design software.
7. S. MALEKI 2000 *Proceedings* 5*th International Conference on Computational Structures Technology*. Scotland: Civil-Comp Press, 177–182. Effect of elastomeric bearings on seismic response of skewed bridges.
8. S. MALEKI 2001 *Proceedings* 1*st MIT Conference on Computational Solid and Fluid Mechanics*. Amsterdam: Elsevier Science. 681–684. Effects of diaphragms on seismic response of skewed bridges.